Contrib Mineral Petrol (2007) 154:591–606
DOI 10.1007/s00410-007-0211-y

ORIGINAL PAPER

The petrogenetic characterization of intermediate and silicic charnockites in high-grade terrains: a case study from southern India

H. M. Rajesh

Received: 3 December 2006 / Accepted: 20 April 2007 / Published online: 26 May 2007

Abstract Large charnockite massifs occur in some of the Precambrian high-grade terrains like the southern Indian granulite terrain. The Cardamom Hill charnockite massif from the Madurai Block, southern India, consists of an intermediate type and silicic type, with the intermediate type showing similarities to high-Ba–Sr granitoids with low K_2O/Na_2O ratios and the silicic type showing similarities to high-Ba–Sr granitoids with high K_2O/Na_2O ratios. Within the constraints imposed by near basaltic composition of the most mafic samples and their relatively high concentrations of both compatible and incompatible elements, comparison with recent experimental studies on various source compositions, and trace- and rare-earth-element modeling, the distinctive features of the intermediate charnockites can be best explained in terms of assimilation–fractional crystallization (AFC) models involving interaction between a mantle-derived basaltic magma and lower crustal materials. Silicic charnockites on the other hand are high temperature melts of moderately hydrous basaltic magmas. A two-stage model which involves an initial partial melting of hydrous basaltic magma and later fractionation explains the geochemical features of the silicic charnockites, with the fractionation stage most probably an open system AFC. It is suggested that for massifs showing spatial association of intermediate and silicic charnockites, a model taking into account their compositional difference in terms of the effect of variations in the conditions (e.g., temperature, water fugacity) that prevailed, can account for plausible petrogenetic scenarios.

Communicated by T.L. Grove.

H. M. Rajesh (✉)
Department of Geology, University of Johannesburg,
Auckland Park Kingsway Campus, P.O. Box 524,
Auckland Park, 2006 Johannesburg, South Africa
e-mail: rajesh.hm@gmail.com

Introduction

Charnockites characterized by orthopyroxene-bearing granitic mineral assemblages are important components of the lower continental crust in many high-grade terrains and usually show a spatial association of rocks differing in modal abundance of the dominant feldspar type (enderbite–charnoenderbite–charnockite; Le Maitre 2002). They have been ascribed to widely divergent origins: granitic rocks metamorphosed to the granulite-facies (metamorphic charnockites; e.g., Newton et al. 1980) and rocks whose pyroxene crystallized directly from a magma (igneous charnockites; e.g., Wendlandt 1981). The scientific literature includes several clearly illustrated examples of spatially associated igneous and metamorphic charnockites (e.g., Limpopo belt, South Africa, Bohlender et al. 1992; Trivandrum block, southern India, Rajesh 2004). Igneous charnockites, usually occurring as large massifs, constitute the dominant variety of charnockite exposed.

A number of studies have addressed the petrogenesis of charnockites associated with mangerites, quartz mangerites, and jotunites in anorthosite–mangerite–charnockite (–granite) (AMCG or AMC) suites, with charnockites and other evolved rocks considered to be residual or cumulates after the removal of a granitic melt (Emslie 1991; Mitchell et al. 1996; Markl and Höhndorf 2003), partial melts of lower crustal granulites (Duchesne et al. 1989; Longhi et al. 1999) or trace-element enriched mantle source (Icenhower et al. 1998), or extensive fractionates of Fe, Ti-rich ferrodiorites (Vander Auwera et al. 1998; Scoates and

Lindsley 2000). However, the petrogenesis of charnockite massifs occurring not part of AMCG/AMC suites, have received little attention, even though they cover substantial portion of many high-grade terrains.

Charnockites occurring in the Neoproterozoic upper amphibolite to granulite-grade terrain of southern India include intrusions of tonalitic–granodioritic–granitic composition occurring over large areas (igneous charnockite massifs), massive metamorphic charnockites showing relict compositional banding and ghost foliation associated with gneissic rocks, and mesoscopic patches and veins of ''arrested'' charnockite (incipient charnockites), representing in situ stages of granulite formation driven by the influx of CO_2-rich fluids (carbonic metamorphism; Newton et al. 1980). This paper assembles geochemical data from a charnockite massif from southern India to discuss and develop an understanding of how geochemical characteristics relate to source rock, petrogenetic process, and tectonic environment. In the process, a classification is suggested for charnockite massifs, which can be of relevance in addressing the petrogenesis of charnockites in high-grade terrains.

Geologic setting

The southern Indian granulite terrain south of Dharwar craton includes several regional *en echelon* Neoproterozoic shear zones which dissect the terrain into different Late Archaean and Proterozoic crustal blocks (Harris et al. 1994; Santosh 1996) (Fig. 1a). While the various crustal scale shear zones within the Palghat–Cauvery shear zone system separates the Madras, Northern, Nilgiri and Madurai blocks, the Achankovil zone in the south separates the Madurai block from the Trivandrum block (Fig. 1a). The northern part of this terrain (the Madras, Northern and Nilgiri blocks) consists primarily of late Archaean to Palaeoproterozoic charnockite massifs (Jayananda and Peucat 1996; Raith et al. 1999; Bhaskar Rao et al. 2003; Mojzsis et al. 2003; Santosh et al. 2003; Ghosh et al. 2004) that forms highland areas interspersed with lowlands consisting of felsic rocks generally in amphibolite facies. Charnockite massifs from the northern part of the Madurai block yield Palaeoproterozoic ages, while those from the southern part yield Mesoproterozoic and Neoproterozoic ages (Bartlett et al. 1995; Jayananda et al. 1995; Miller et al. 1996; Santosh et al. 2003; Ghosh et al. 2004). This study concentrates on the Cardamom Hill charnockite massif within the Madurai Block (Fig. 1).

The Madurai block covers the largest portion of the southern Indian granulite terrain and represents a composite mid- to lower-crustal domain. Large parts of the Madurai block are made up of charnockite massifs, which form the highlands of the Western Ghats. To the east, in the lowlands, hornblende-biotite gneisses, quartzofeldspathic biotite gneisses, minor metasedimentary rocks (quartzites, calc-silicates, marbles, pelitic to psammitic granulites), as well as large granite intrusives are exposed. Numerous enclaves and rafts of migmatized garnet–cordierite–sillimanite gneisses occur in the lowlands south of the Palni–Kodaikanal Hills massif. A number of anorthosite massifs, including the Odanchantram massif, occur northeast of the Palni–Kodaikanal Hills massif, and is associated with younger pink granites. Intercalated sapphirine, corundum and kornerupine bearing lithologies (mostly aluminous granulites) have been reported from a number of localities in the central and northern parts of this block (Grew 1984; Lal et al. 1984; Mohan and Windley 1993; Raith et al.

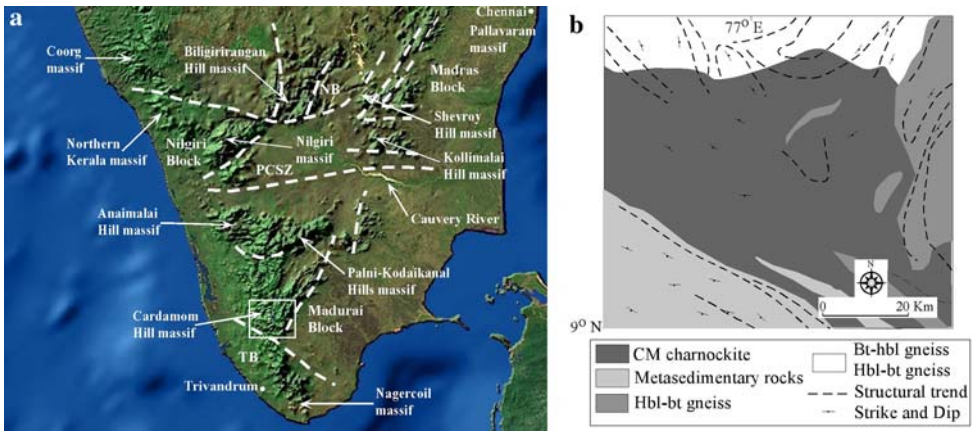

Fig. 1 **a** Shaded relief image of southern India showing the distribution of major charnockite massifs including the Cardamom hill massif. The different crustal blocks are also shown. *TB* Trivandrum Block; *NB* Northern Block; *PCSZ* Palghat Cauvery Shear Zone system. *Rectangle* indicates the area covered in **b**. **b** Geologic map of the Cardamom Hill massif and surroundings. Approximate sampling location of intermediate (*dark circles*) and silicic (*white circles*) charnockites are also shown

1997; Koshimoto et al. 2004) providing robust evidence for ultrahigh temperature metamorphism. Recent studies from Madurai block have suggested a polymetamorphic and multistage *P–T* (700–1,000°C and 5–12 kbar; Harris et al. 1982; Mohan and Windley 1993; Raith et al. 1997; Satish-Kumar et al. 2002; Koshimoto et al. 2004; Sajeev et al. 2004) evolution for the terrane.

Salient features of the Cardamom Hill charnockite massif

Most exposed rocks of the Cardamom Hill charnockite massif are grouped into intermediate type and silicic type. CESS (2004) reported early- and late-Neoproterzoic ages (U–Pb zircon and EPMA monazite ages) for the intermediate and silicic charnockites from the Cardamom Hill massif. Miller et al. (1996) reported a U–Pb zircon age of 588 ± 6 Ma for the silicic charnockite.

The term intermediate is used here to refer to charnockites having lower K-feldspar contents, greater mafic mineral contents (hence darker in appearance) and low SiO_2 (see next section), while silicic type refers to comparatively less dark charnockites with higher SiO_2 (see next section). Both types usually appear dark greenish-gray, homogenous, and massive in quarry exposures. Some of the exposures show a migmatitic gneissic overprint with a foliation trending NW–SE–NE–SW, imparted by biotite, and signs of retrogression (retrogressed portions are lighter in color). Their igneous parentage is evident from the homogeneity at outcrop scale, presence of enclaves, in-situ development of ±orthopyroxene bearing pegmatoids, granitic textures, observed order of crystallization of primary minerals, as well as distinct chemical features (see next section).

Metasedimentary rocks in the south and hornblende–biotite gneiss/biotite–hornblende gneiss in the north, bound the Cardamom Hill massif (Fig. 1b). The gneissic exposures in the south show variations from quartzofeldspathic garnet–biotite gneiss to migmatitic garnet gneiss to cordierite gneiss. Irregular patches of both large- and small-scale incipient charnockites are spectacularly developed in many of the migmatitic garnet–biotite gneiss exposures (e.g., see Rajesh 2004). The ortho-gneisses in the north range in composition from granodiorite with up to 12% modal biotite, to tonalite with up to 8% biotite, to alkali feldspar granite with less than 5% modal biotite. Biotite-rich granitoid is much more common than hornblende-rich granitoid.

The most commonly encountered mineral assemblage of silicic type charnockite is qtz–kfs–plg–opx–mt–il–zr–ap ± hbl ± bt. The intermediate type charnockite is distinguished from the silicic type by its relatively low K-feldspar content, greater mafic mineral content and the occurrence of clinopyroxene. Compositionally the intermediate type ranges from diorite to quartz monzodiorite, while the silicic type ranges from granodiorite to monzogranite in the normative Qz–Or–Ab + An ternary plot. In the *Q–P* cationic classification of Debon and Le Fort (1988), they show a similar compositional range, with the exception of the most silicic samples that fall in the granite field; the overall trend of intermediate charnockite is calc-alkaline, while that of silicic charnockite is tholeiitic.

Whole-rock chemical variations

Representative geochemical data of the Cardamom Hill charnockites are given in Table 1. Major and trace element contents of the charnockite samples were determined by a Rigaku RIX-2000 X-ray fluorescence spectrometer (Fukuoka University of Education, Japan) on glass beads. Volatiles were determined by loss on ignition. Representative charnockite samples were analysed for REEs by ICP-MS (Plasma Quad PQ1) on trace element solutions after separation of major elements through ion-exchange resins. The operating parameters and analytical precision are illustrated in Balaram et al. (1996) and the references therein. Chacko et al. (1992) presented geochemical data on the Cardamom Hill charnockites and is included in the various geochemical plots together with the data from this study.

The intermediate charnockite (~53–60 wt%) is characterized by higher TiO_2, total Fe (as Fe_2O_3), MnO, MgO, CaO, P_2O_5, and lower K_2O, Ba, Rb/Sr, Zr, La, Ce, than the silicic charnockite (~65–71 wt%). Na_2O and Al_2O_3 show an increasing trend with silica for the intermediate charnockite, while they show a decreasing trend for the silicic charnockite (Fig. 2). The intermediate and silicic charnockites have different K_2O/Na_2O ratios (intermediate charnockite: 0.23–0.82; silicic charnockite: 0.79–2.76; Fig. 3a). In terms of Fe-number, intermediate charnockite samples are magnesian, while silicic charnockite samples are magnesian to ferroan (Fig. 3a). Although intermediate charnockite samples show tightly grouped calc-alkalic affinity in terms of modified alkali-lime index, silicic charnockite samples show variations from calc-alkalic to alkali-calcic (Fig. 3b). In terms of alumina saturation index (ASI), intermediate charnockite is predominantly metaluminous while silicic charnockite is metaluminous to slightly peraluminous (Fig. 3b).

The Cardamom Hill charnockite massif is rich in Ba and Sr, similar to high-Ba–Sr granitoids (Tarney and Jones 1994), with the intermediate type showing similarities to high-Ba–Sr granitoids with low K_2O/Na_2O ratios, while the silicic type shows similarities to high-Ba–Sr granitoids with high K_2O/Na_2O ratios. Ba and Rb follow the K_2O

Table 1 Representative major and trace element analyses of the Cardamom Hill charnockite samples

Rock type	Inter CM	Inter CM	Inter CM	Inter CM	Inter CM	Inter CM	Silicic CM	Silicic CM	Silicic CM	Silicic CM	Silicic CM	Silicic CM
Major elements (wt%)												
SiO_2	53.14	54.41	55.01	55.98	56.31	58.43	65.04	67.14	67.44	67.8	68.72	71.01
TiO_2	2.06	1.55	1.34	1.62	1.28	0.82	0.57	0.45	0.51	0.29	0.6	0.48
Al_2O_3	15.31	14.74	17.01	16.11	16.38	16.03	16.11	14.8	14.81	15.32	14.61	14.3
Fe_2O_3*	10.14	9.01	7.98	8.97	8.36	7.68	4.33	4.6	4.52	3.49	3.75	3.13
MnO	0.172	0.145	0.166	0.148	0.13	0.128	0.127	0.066	0.081	0.068	0.066	0.057
MgO	4.88	4.86	3.78	4.41	4.01	4	1.86	1.63	1.02	2.16	1.17	0.51
CaO	8.01	7.98	6.41	6.42	6.24	5.31	3.62	2.9	2.7	2.97	2.4	1.02
Na_2O	3.4	3.61	4.21	3.57	4	3.6	3.61	3.98	3.62	2.97	3.42	2.21
K_2O	1.54	2.1	1.6	1.98	2.24	2.26	4.03	3.74	4.17	4.2	5.21	6.11
P_2O_5	0.92	0.76	0.64	0.62	0.56	0.57	0.32	0.28	0.32	0.27	0.2	0.12
Total	99.57	99.17	98.15	99.83	99.51	98.83	99.62	99.59	99.19	99.54	100.15	98.95
K_2O/Na_2O	0.45	0.58	0.38	0.55	0.56	0.63	1.12	0.94	1.15	1.41	1.52	2.76
ASI	0.74	0.68	0.87	0.85	0.83	0.92	0.98	0.95	0.99	1.06	0.95	1.20
Agpaitic Index	0.47	0.56	0.51	0.50	0.55	0.52	0.64	0.72	0.71	0.62	0.77	0.72
MALI	–3.07	–2.27	–0.60	–0.87	0.00	0.55	4.02	4.82	5.09	4.20	6.23	7.30
Fe-number	0.68	0.65	0.68	0.67	0.68	0.66	0.70	0.74	0.82	0.62	0.76	0.86
Trace elements (ppm)												
Ba	890	1040	720	985	1230	1290	1180	1400	1530	1830	1720	2080
Rb	48	64	46	68	84	85	108	110	128	118	141	155
Sr	723	604	511	613	501	484	404	405	378	311	332	289
Zr	164	138	187	206	248	254	264	308	312	287	352	414
V	48	50	108	123	148	134	152	124	112	77	52	42
Cr	254	221	228	206	152	148	150	111	100	108	75	85
Ni	88	72	53	55	41	42	25	18	20	17	10	11
Rb/Ba	0.05	0.06	0.06	0.07	0.07	0.07	0.09	0.08	0.08	0.06	0.08	0.07
Rb/Sr	0.07	0.11	0.09	0.11	0.17	0.18	0.27	0.27	0.34	0.38	0.42	0.54
K/Rb	265.99	272.04	288.37	241.41	221.09	220.44	309.37	281.89	270.10	295.09	306.35	326.82
K/Ba	14.35	16.74	18.42	16.67	15.10	14.52	28.32	22.15	22.60	19.03	25.11	24.35
C.I.P.W. Norm												
q	8.20	6.86	8.03	10.31	8.29	13.64	19.07	22.15	24.22	25.75	22.85	32.51
or	9.14	12.51	9.63	11.72	13.3	13.51	23.91	22.19	24.84	24.94	30.74	36.49
ab	28.89	30.80	36.30	30.26	34.01	30.82	30.66	33.82	30.88	25.25	28.90	18.90
an	22.06	17.96	23.22	22.12	20.22	21.15	15.91	11.52	11.40	13.03	9.11	4.32
di	4.12	9.41	0.65	0.51	2.52							
hy	10.30	7.85	9.29	10.77	8.87	10.08	4.65	4.08	2.56	5.41	2.91	1.28
il	0.37	0.31	0.36	0.32	0.28	0.28	0.27	0.14	0.17	0.15	0.14	0.12
hm	10.18	9.09	8.13	8.99	8.4	7.77	4.35	4.62	4.56	3.51	3.74	3.16
ap	2.14	1.78	1.51	1.44	1.3	1.34	0.74	0.65	0.75	0.63	0.46	0.28

ASI Alumina saturation index; *MALI* modified alkali lime index (Na_2O+K_2O-CaO); Fe-number – Fe_2O_3*/(Fe_2O_3*+MgO)

[a] Total Fe as Fe_2O_3

trend of increasing abundance with SiO_2, while Sr decreases with differentiation for the charnockite samples. The silicic charnockite has higher Rb/Sr ratios (~0.20–0.77) in comparison to the intermediate charnockite (~0.05–0.22). On the other hand, intermediate charnockite has higher Sr/Y ratio (~15–22) than the silicic charnockite (~4–9). The K/Rb ratios of Cardamom Hill charnockite samples (intermediate charnockite: ~170–288, silicic charnockite: ~240–327) fall in the range of K/Rb ratios of low–medium pressure charnockites (~200–500) and differ

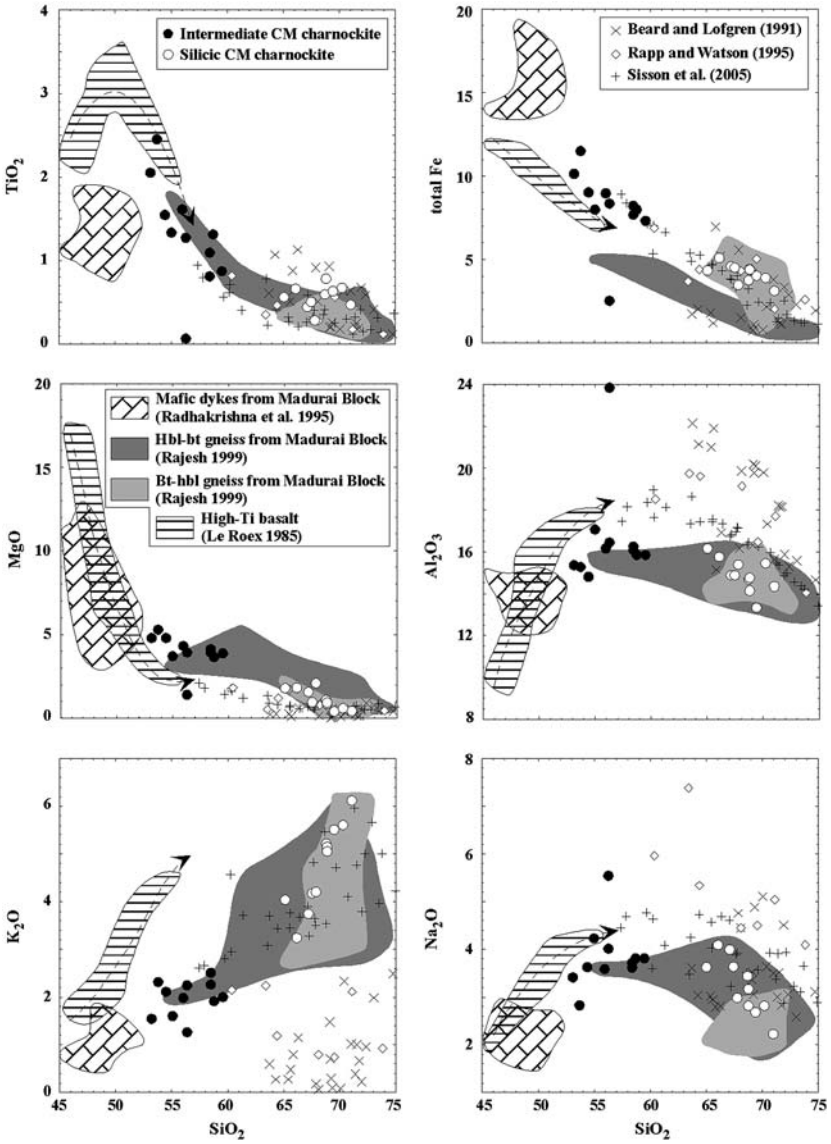

Fig. 2 Representative major element variation diagrams of the Cardamom Hill (CM) charnockite samples. The compositional ranges of mafic dykes, hbl–bt gneiss and bt–hbl gneiss from the Madurai block are shown to aid in the petrogenetic characterization of charnockites. Quantitative modeled trends of possible fractional crystallization of a high-Ti basalt, amphibole dehydration melts (only those with comparable *P–T* conditions with the intermediate charnockites are plotted) from Beard and Lofgren (1991) and Rapp and Watson (1995), and high temperature hydrous basalt melts from Sisson et al. (2005) are also shown

from those of high-pressure charnockites (>1,000) from southern India (Condie and Allen 1984). Rare earth element patterns are LREE enriched (La_N/Yb_N: intermediate charnockite ~6–12, silicic charnockite ~10–18; Ce_N/Yb_N: intermediate charnockite ~3–8, silicic charnockite ~8–11) relative to the heavy REE with a negative Eu anomaly [Eu/Eu* = 0.18–0.35 (intermediate charnockite), 0.23–0.31 (silicic charnockite)]. In the normative An–Ab–Or triplot, intermediate charnockite compositions fall mainly in the tonalite field, while the silicic charnockite compositions fall in the granodiorite–granite field (Fig. 3c). The different geochemical characteristics of the intermediate and silicic charnockites are compiled in Table 2.

Crystallization temperatures of ~1,000°C are supported by the high P_2O_5 and TiO_2 contents of the intermediate charnockite samples (~1 and ~2.5 wt%, respectively; Harrison and Watson 1984; Green and Pearson 1986; Fig. 4). Silicic charnockite samples have a lower crystallization temperature (~900°C; Fig. 4). In the Q–Ab–Or system, intermediate charnockite samples occur towards the Ab corner parallel to the Q–Ab sideline while the silicic charnockite samples spread around the minimum. The shift of the minima from intermediate charnockite towards the Q–Or sideline allows more potassic non-minimum melts (silicic charnockite) to be generated.

A continental arc tectonic setting was suggested for the Cardamom Hill charnockites by Rajesh (1999) and is supported by the application of tectonic discrimination diagrams of Verma et al. (2006) (Fig. 5). Verma et al. (2006) proposed four pertinent discriminant function diagrams, based on $\log_e$-transformation of concentration ratios of major-elements—a technique recommended for a correct statistical treatment of compositional data, to discriminate four tectonic settings: island arc, continental

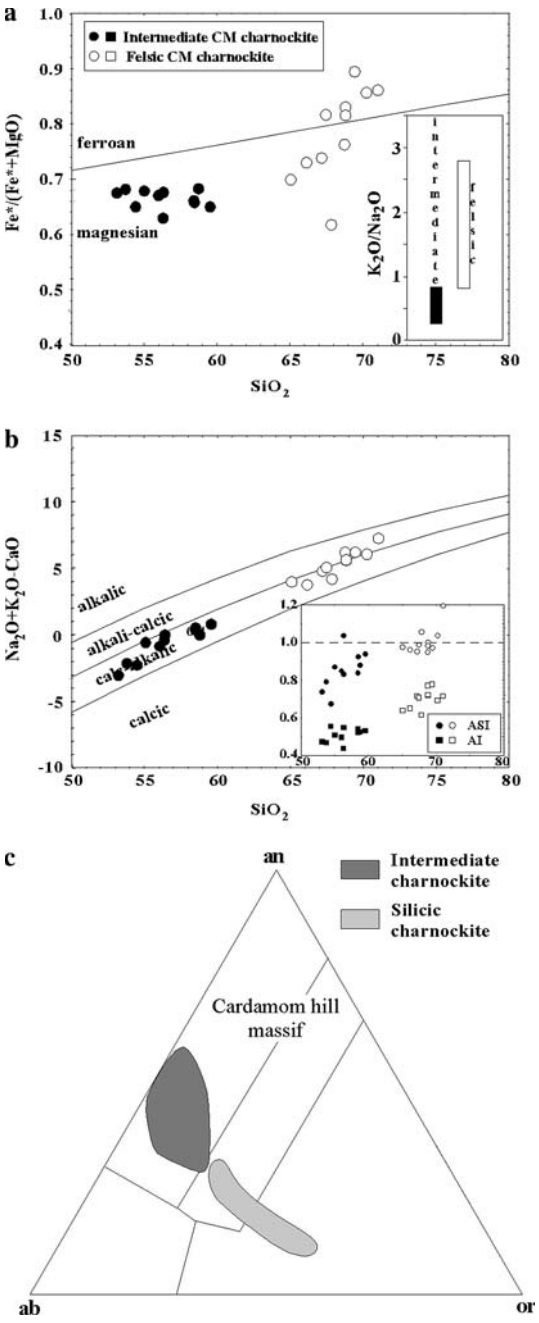

Fig. 3 Na_2O+K_2O–CaO versus SiO_2 (**a**), Fe*/Fe*+MgO versus SiO_2 (**b**), and normative An–Ab–Or ternary (**c**) plots of the Cardamom Hill (CM) charnockite samples. The ferroanmagnesian and calcic–calc-alkalic–alkalicalcic–calcic discrimination is from Frost et al. (2001). *Inset* in (**a**) is a *bar diagram* illustrating the variation in K_2O/Na_2O ratios, while *inset* in (**b**) illustrates the variation of aluminium saturation index (ASI) and agpaitic index (AI) of intermediate and silicic charnockites

rift, ocean-island, and mid-ocean ridge. Although the diagrams are intended for use with basic and ultrabasic rocks, the Cardamom Hill charnockites fall in the island arc field (Fig. 5), similar to continental arc rocks illustrated in Verma et al. (2006).

Petrogenetic characterization

Nature of the source rock and petrogenetic process

Viable models for the genesis of charnockites, like the Cardamom Hill massif, include high temperature melting of Ti-enriched mantle-derived underplates compositionally similar to high-Ti continental flood basalts (Kilpatrick and Ellis 1992), fractionation of primitive mantle-derived water-undersaturated magmas followed by high-temperature crystallization (fractional crystallization of arc basalts; Eggins and Hensen 1987), or mixing of variably hydrous mantle-derived basalt and crustal components (AFC-type: Sheraton et al. 1992; MASH-type: Emslie and Hunt 1990).

The crustal source rocks present in the basement of Cardamom Hill and surrounding areas include mafic and granodioritic orthogneiss, and pelitic gneiss. Melting of a pelitic source usually produces peraluminous melts. Montel and Vielzeuf (1997) showed that the K_2O/Na_2O ratio of melts from a pelitic source is significantly higher (average 4–24), in comparison to the ratio of the least evolved samples from the Cardamom Hill charnockites. Although major element characteristics of the surrounding tonalitic–granodioritic gneisses (see Fig. 2) are comparable with the Cardamom Hill charnockites, ratios of incompatible elements are higher in gneisses than the Cardamom Hill charnockites (e.g., Fig. 6) contrary to what is expected during crustal anatexis. These ratios rule out derivation of the Cardamom Hill charnockites by melting of tonalitic–granodioritic gneisses.

Eggins and Hensen (1987) suggested that the hot, dry and isotopically primitive mantle-derived nature of augite-hypersthene granodiorites, from the Barrington Tops batholith, eastern Australia, is most adequately explained by the fractional crystallization of basalt. This process would be difficult to detect geochemically if it occurred at a pressure below that required for the formation of garnet. When plotted in Harker diagrams, the possibility of simple fractional crystallization is not fully compatible with modeled [using the MIX3, an updated version of the program described in Nielsen (1990)] fractionation trends in major and trace element abundances from a high-Ti basalt (Le Roex 1985) to the Cardamom Hill charnockites (see Fig. 2). Fractional crystallization might be responsible for contrasts among the intermediate and silicic charnockites. This would explain, for example, the decrease in Eu/Eu^*_N and increase in REE abundances that correlate with increasing SiO_2. Alternatively, such contrasts may reflect differences in the degree of melting with lower degree melts having higher SiO_2 and higher REE contents. It should be noted that, at constant values of partition coefficients, fractional crystallization is less efficient than partial melting in changing rates of incompatible trace elements with different degrees

Table 2 Comparison of geochemical characteristics of intermediate and silicic charnockites from the Cardamom Hill massif

Geochemical characteristic	Intermediate charnockite	Silicic charnockite
SiO_2	Low (~53–60)	High (~65–71)
TiO_2	High (~0.8–2.5)	Low (~0.3–0.77)
K_2O/Na_2O	Low (~0.23–0.82)	High (~0.79–2.76)
Fe-number	Magnesian	Magnesian to ferroan
Modified alkali lime index	Calc-alkalic	Calc-alkalic to alkali-calcic
Alumina saturation index	Metaluminous	Metaluminous to slightly perlauminous
Agpaitic index	Low (~0.47–0.56)	High (~0.62–0.77)
Normative Ab/An	Low (~1.31–1.71)	High (~1.93–4.38)
Rb/Sr	Low (~0.05–0.22)	High (~0.20–0.77)
Sr/Y	High (~15–22)	Low (~4–9)
K/Rb	Low (~170–288)	High (~240–327)
La_N/Yb_N	Low (~6–12)	High (~10–18)
Ce_N/Yb_N	Low (~3–8)	High (~8–11)
Eu/Eu*	Low (~0.18–0.35)	High (~0.23–0.31)

Fe-number – total Fe/(total Fe + MgO); Modified alkali lime index – $Na_2O + K_2O$–CaO

of incompatibility (Hanson 1978). Therefore, the variation in incompatible element ratios between the intermediate and silicic charnockites (e.g., La/Lu) is most consistent with later fractional crystallization.

Various high-temperature and high-pressure experiments on partial melting of basaltic material showed that La_N/Yb_N and Sr/Y values are mainly controlled by the relative abundances of garnet, clinopyroxene, amphibole and plagioclase in the residue; the more amphibole and plagioclase and lesser amounts of garnet in the residue, the lower the La_N/Yb_N and Sr/Y values in the melt (e.g., Rapp et al. 1991; Springer and Seck 1997). The lower La_N/Yb_N and Sr/Y values of the Cardamom Hill charnockite samples are comparable to melts derived from garnet-free amphibolitic sources, and contrasts those derived from garnet-bearing ecologitic sources (high Sr/Y and low Y values, because of the partitioning of Y into residual garnet; see Martin 1987) (Fig. 7). This together with the observed LILE-enrichment in the Cardamom Hill charnockites suggests an enrichment of amphibole and plagioclase in the residue. Therefore, partial melting must have occurred at high temperatures in the stability field of plagioclase at approximately 900–1,100°C (Rapp et al. 1991; Springer and Seck 1997), consistent with thermometry observations for the Cardamom Hill charnockites (Fig. 4). Garnet was absent in melting experiments conducted at 8 kbar (Rushmer 1991; Rapp et al. 1991) and present in those conducted at 10 kbar (Wolf and Wyllie 1994), but the location of the garnet-in curve is composition dependent. On that basis, it is argued that the Cardamom Hill charnockites were generated at pressures of <8 kbar. Although unlikely, they could have been generated at pressures up to 10 kbar, as garnet may be totally consumed during melting at temperatures of 1,000°C (Wolf and Wyllie 1994).

Petford and Gallagher (2001) showed that more mafic lower SiO_2 melt compositions can be produced by higher degrees of partial melting of amphibolite protolith, with lower average melt fractions, and more silica-rich liquids formed at smaller degrees of partial melting (see Fig. 7c). However, such variation in the degree of melting is not consistent with sub-equal abundances of incompatible elements (such as Ba, Rb, K, and La) observed in the intermediate and silicic charnockites from the Cardamom Hill massif. It is therefore probable that the mineralogical and geochemical difference between intermediate and silicic charnockites is produced by different petrogenetic processes.

Origin of the intermediate charnockites

If dehydration melting did produce the intermediate charnockites, there is not likely to be any amphibole in the residue. Further a comparison with melts derived from basaltic dehydration melting experiments at mid- to lower-crustal pressures indicate that the composition of intermediate charnockites overlap only the highest *T* basaltic dehydration melts and many intermediate charnockites (especially the less siliceous and produced at *T* well in excess of 1,000°C) are more mafic than any reported dehydration melts (Fig. 8). Ferrodiorite is probably a more likely protolith for the petrogenesis of charnockites by crustal melting than basalt (Duchesne et al. 1989) because it has a lower melting point than basalt. Scoates et al. (1996), however, showed experimentally that melts of ferrodioritic source compositions are monzonitic, different from the Cardamom Hill charnockites.

The most mafic samples of the intermediate charnockites are nearly basaltic in composition and have relatively

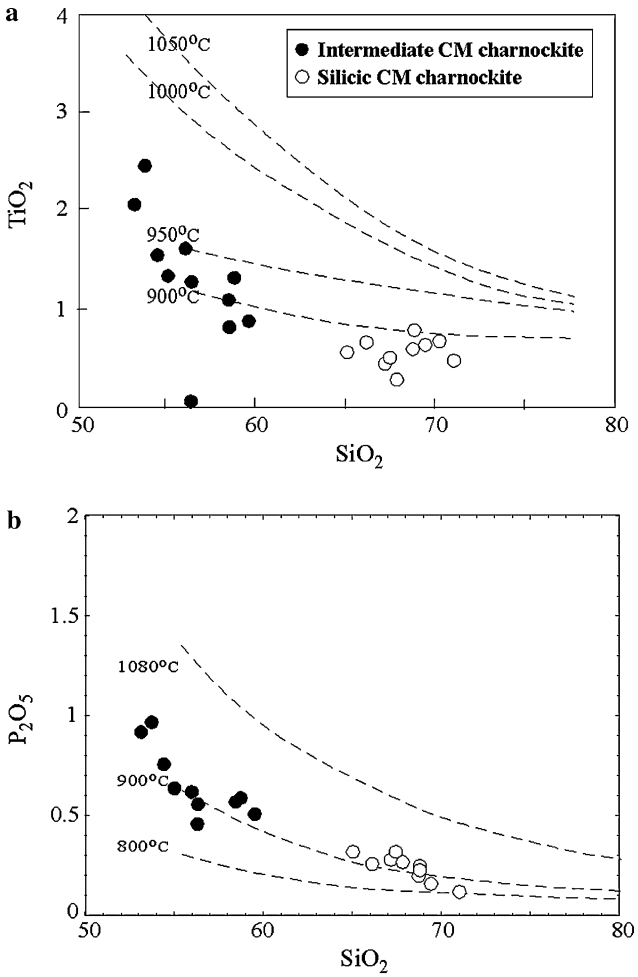

Fig. 4 **a** TiO_2 versus SiO_2 and **b** P_2O_5 versus SiO_2 plots of the Cardamom Hill (CM) charnockite samples. The isotherms in (**a**) show Fe-Ti oxide saturation temperatures at 7.5 kbar (Green and Pearson 1986), while those in (**b**) illustrate apatite saturation temperatures at 7.5 kbar (Harrison and Watson 1984)

high concentrations of both compatible and incompatible elements. Assimilation–fractional crystallization (AFC) models involving interaction between a mantle-derived basaltic magma and lower crustal materials may be a plausible way to generate the intermediate charnockites, especially considering the occurrence of early Proterozoic (~2.0 Ga) mafic dykes with geochemical characteristics of tholeiitic basalts (Radhakrishna et al. 1995) in the Madurai block. An assimilation model can certainly account for the high concentrations of both compatible and incompatible elements (Fig. 9a, b). The AFC models (involving the mafic dykes and hbl–bt gneisses from the Madurai Block) of the most incompatible elements do reproduce trends for the Cardamom Hill intermediate charnockite. The best-fit models require assimilation/fractional crystallization ratios (r) to be 0.5 or greater (Fig. 9c, d). For bulk assimilation where crystalline components of the assimilant are resident in the magma, such high r can be accounted for.

The effectiveness of any assimilation process is essentially constrained by the thermal budget of the assimilating magma and the fertility of the wall rock contaminant (Marsh 1989). The long-held view that the assimilated mass cannot surpass the amount of crystallized cumulate because of thermal constraints has been challenged by thermodynamic studies of Reiners et al. (1995), which suggest the possibility of r factors substantially greater than one. However, such large factors are restricted to basaltic magmas during a narrow isenthalpic AFC interval, and only when intruded into preheated upper crustal lithologies. If, instead of entirely melting the country rock or even partially melting them and extracting melts, country rocks are incorporated in toto, melt, crystals, and all into host magmas, heat requirements for assimilation are significantly reduced (Grove et al. 1988). Reactive bulk assimilation involving (1) incorporation, heating, and dehydration melting of country rock fragments in the melt, (2) disaggregation and disintegration of the partially molten fragments into the host magma, and (3) reactions that are essentially the reverse of dehydration melting reactions (hydration–crystallization reactions; Beard et al. 2004) yielding amphibole and/or mica, provides a likely mechanism to explain the higher r, which is difficult to conceive if assimilation requires complete melting (Beard et al. 2005). Because the crustal rocks need heat both to raise their temperature from ambient to their solidus and for fusion, hotter crustal rock temperatures in excess of 600°C can lead to more efficient assimilation. The high r values required to explain the AFC model for intermediate charnockites is supported by recent lower crustal temperature estimates (~900°C) from the Madurai Block (e.g., Koshimoto et al. 2004). Further, as assimilation increases the magma mass and also the mass of the subsequent crystallization, the AFC process might have started at the very beginning of differentiation to result in high degrees of assimilation.

Fractional crystallization (which must occur as a consequence of assimilation of crust, especially in relatively fluid basaltic magmas), involving plagioclase, can account for the decrease in Sr abundances and strong negative Eu anomalies of the intermediate charnockite samples. To further constrain the possibility of AFC, the composition of intermediate charnockites was compared with reaction curves calculated by Patiño Douce (1999) to model the composition of melts that would be produced by interaction of a putative crustal melt end member with a basaltic melt. The trend of the intermediate charnockite samples generally follows the model reaction curves and fall between the high and low pressure curves (Fig. 10). The area between the high and low pressure curves in Fig. 10 encompasses the range of depths at which mantle–crust interactions are most likely to take place leading to the formation of

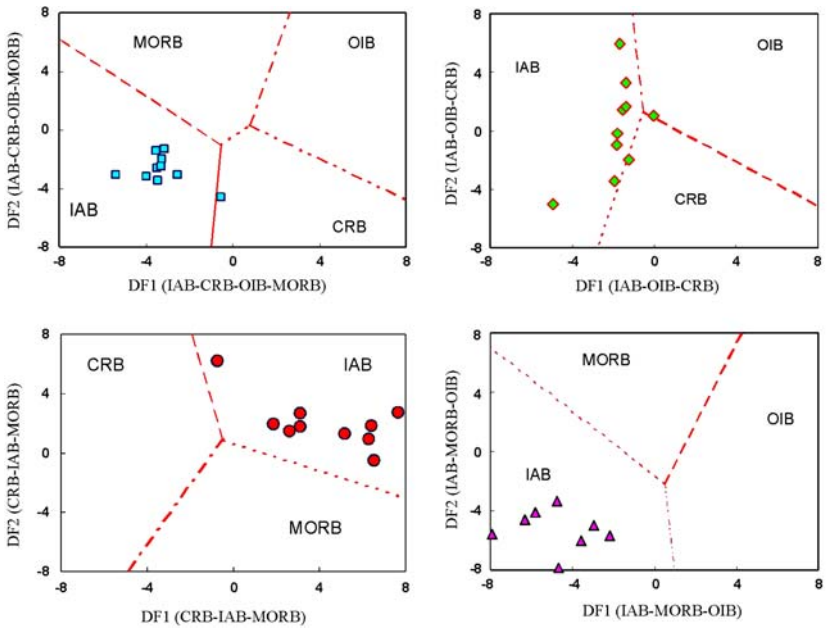

Fig. 5 IAB–CRB–OIB–MORB, IAB–OIB–CRB, CRB–IAB–MORB, and IAB–MORB–OIB diagrams illustrating the possible tectonic setting of the Cardamom Hill charnockites. The base diagrams are from Verma et al. (2006) to discriminate four tectonic settings: island arc (IAB), continental rift (CRB), ocean-island (OIB), and mid-ocean ridge (MORB). The two discriminant functions, DF1 and DF2, are: DF1 = –4.6761·ln(TiO_2/SiO_2)adj + 2.5330·ln(Al_2O_3/SiO_2)adj – 0.3884·ln(Fe_2O_3/SiO_2)adj + 3.9688·ln(FeO/SiO_2)adj + 0.8980·ln(MnO/SiO_2)adj – 0.5832·ln(MgO/SiO_2)adj – 0.2896·ln(CaO/SiO_2)adj – 0.2704·ln(Na_2O/SiO_2)adj + 1.0810·ln(K_2O/SiO_2)adj + 0.1845·ln(P_2O_5/SiO_2)adj + 1.5445, and DF2 = 0.6751·ln(TiO_2/SiO_2)adj + 4.5895·ln(Al_2O_3/SiO_2)adj + 2.0897·ln(Fe_2O_3/SiO_2)adj + 0.8514·ln(FeO/SiO_2)adj – 0.4334·ln(MnO/SiO_2)adj + 1.4832·ln(MgO/SiO_2)adj – 2.3627·ln(CaO/SiO_2)adj – 1.6558·ln(Na_2O/SiO_2)adj (See Verma et al. 2006 for details)

granitoids (Patiño Douce 1999). Thus it is suggested that assimilation–fractional crystallization processes played an important role in the formation of intermediate charnockites from the Cardamom Hill massif.

Origin of the silicic charnockites

The chemical composition of silicic charnockites from the Cardamom Hill massif are depleted in total alkalis, enriched in lime and have relatively constant ratio of alumina to ferromagnesian components (~2–4) comparable to amphibolite-derived melts. However, unlike the low-K silicic melts produced by the dehydration melting experiments, the least evolved silicic charnockite samples have medium-K contents, with evolved samples having higher K_2O contents. Further, basalt dehydration melting yields lesser quantities of silicic liquids. A survey of the various amphibolite dehydration and water-saturated melting experiments shows that water-saturated systems melt at lower temperatures than the fluid-absent equivalents, and tend to produce higher melt fractions (up to 60–70%; Beard and Lofgren 1991; Rushmer 1991; Wolf and Wyllie 1994). In this context, medium- to high-K melts produced by high-temperature melting of moderately hydrous medium-K basaltic compositions by Sisson et al. (2005) assume significance.

The K/Na ratio of the source material strongly influences the ratio in the resulting partial melts (e.g., Helz 1976; Beard and Lofgren 1991). The silicic liquids produced from most basalt dehydration melting experiments (with low-K starting materials) have low-K_2O contents (e.g., Beard and Lofgren 1991). There are few exceptions, like Rapp and Watson (1995), who produced medium-K silicic liquids at higher temperatures (~1,050°C). Here the temperature condition is probably too high for the estimates obtained for Cardamom Hill silicic charnockites. In terms of total alkali contents, the least evolved silicic charnockite samples closely resemble high-temperature (900–950°C) hydrous basalt melts from Sisson et al. (2005), than melt compositions from basaltic rocks with little or no water. To evaluate this further, a comparison of melt compositions from Beard and Lofgren (1991) (BL91), Rapp and Watson (1995) (RW95) and Sisson et al. (2005) (S05), with the Cardamom Hill silicic charnockite samples was attempted.

In Harker diagrams (see Fig. 2), silicic liquids from BL91 have higher TiO_2, Al_2O_3 and CaO contents, and lower Na_2O and K_2O contents than the silicic charnockite

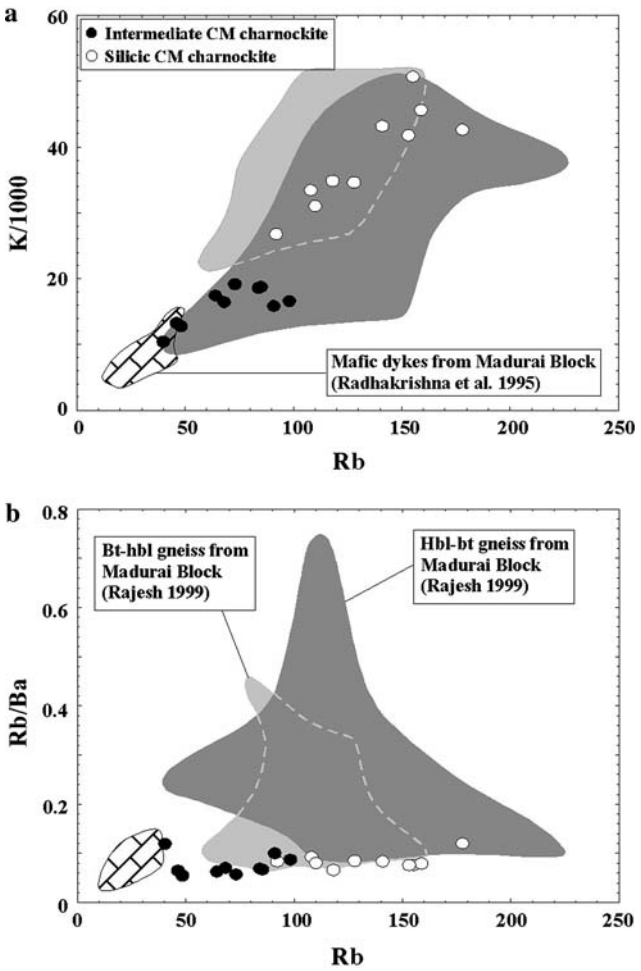

Fig. 6 **a** K/1000 versus Rb and **b** Rb/Ba versus Rb plots of the Cardamom Hill (CM) charnockite samples. The compositional ranges of mafic dykes and hbl-bt gneiss and bt-hbl gneiss from the Madurai block are also shown

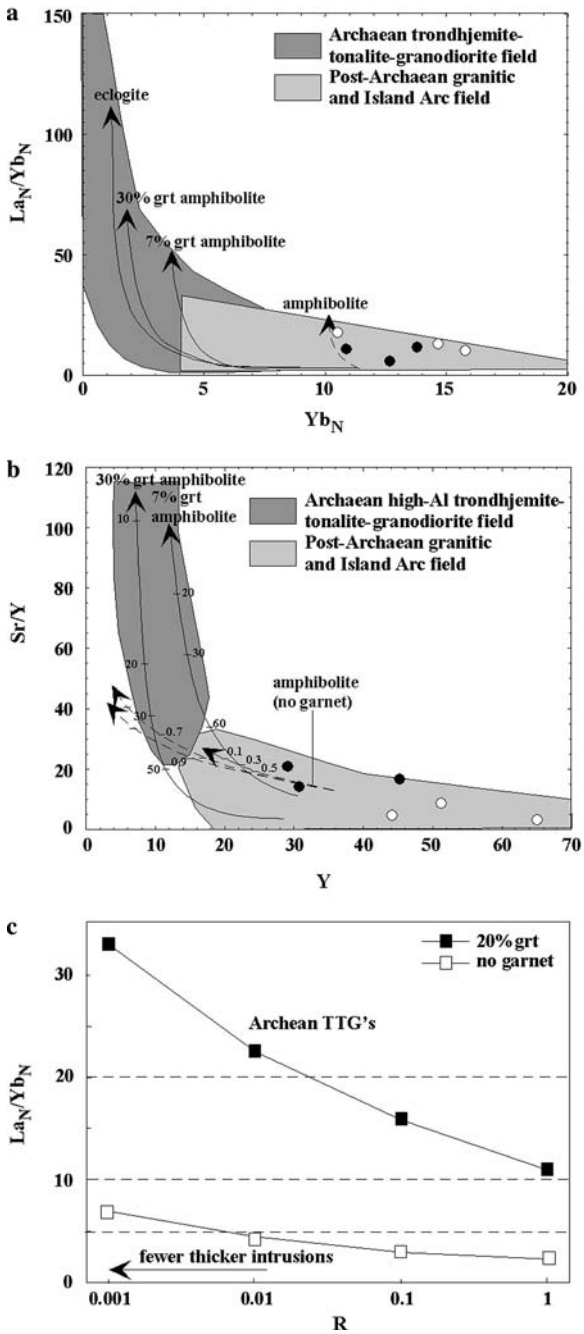

Fig. 7 **a** La_N/Yb_N versus Yb_N and **b** Sr/Y versus Y plots of the Cardamom Hill charnockite samples. Fields in **a** and **b** are from Martin (1986) and Drummond and Defant (1990). Batch partial melting trends from a continental basalt source with mineralogies of eclogite, garnet-free amphibolite, and amphibolite with 7 and 30% garnet are shown in (**a**) (Petford and Atherton 1996). Partial melting curves expected for garnet-free amphibolitic and garnet-bearing eclogitic residues are shown in (**b**) (Martin 1987). **c** Modeled La/Yb_N ratios of partial melts from a garnet-free and garnet-bearing amphibolite protoliths as a function of degree of melting (Petford and Gallagher 2001). Each point represents a discrete melting event, with fewer, thicker intrusions ($R < 1$) giving rise to higher calculated La/Yb ratios due to smaller partial melt volumes in the model liquid despite the source mineralogy staying constant [see Petford and Gallagher (2001) for details]

samples. In contrast, silicic liquids from RW95 show closer resemblance to the silicic charnockite samples than BL91. But Na_2O and Al_2O_3 contents are higher in RW95 melts than the silicic charnockite samples. Further the silicic charnockite samples have higher K_2O contents than the RW95 melts. Clearly the high-temperature melts from S05 show the closest resemblance to the silicic charnockite samples than BL91 and RW95. In terms of alumina saturation index, high temperature hydrous basalt melt compositions from S05 vary from metaluminous to slightly peraluminous, similar to the silicic charnockites. Melts from RW95 and BL91 are peraluminous. Only at very high degrees of partial melting, i.e. at temperatures above 1,000°C, dehydration melts produced from basaltic sources start to become metaluminous (e.g., Rapp et al. 1991; Rapp and Watson 1995). As outlined in earlier sections, such high temperatures were most probably not reached in the Cardamom Hill silicic charnockites. Thus high-temperature

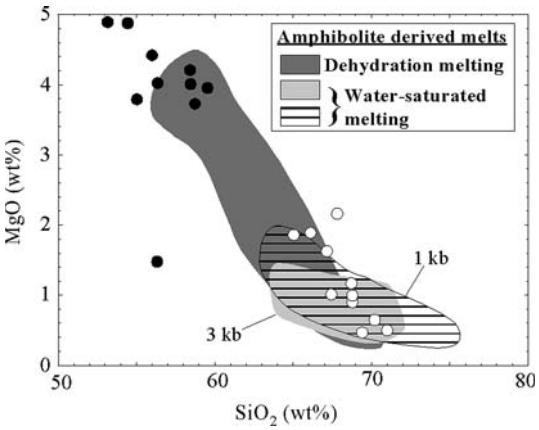

Fig. 8 MgO versus SiO_2 plot illustrating the comparison of the Cardamom Hill charnockite compositions with glasses produced by melting of greenstone and amphibolite at different fH_2O. Glass analyses [dehydration melting at 950–1,000°C, mid- to lower-crustal pressures; water-saturated melting at 1 and 3 kb P_{total}] are from Beard and Lofgren (1991), Rushmer (1991), and Wolf and Wyllie (1989)

melting of a moderately hydrous basaltic composition is suggested as a possible model to explain the formation of silicic charnockites from the Cardamom Hill massif.

Plagioclase fractionation could account for the Sr depletion and Eu anomaly observed in the silicic charnockite samples with differentiation. Simple Rayleigh fraction models indicate that the silicic magmas must undergo ~10–20% fractional crystallization of plagioclase to produce the observed Eu anomaly. Obviously, the amount of crystallization may be significantly less if it was accompanied by addition of crustal material with low Eu/Eu* ratios. A combined fractional crystallization and partial melting model of a hydrous basaltic source is illustrated in terms of Rb and Sr in Fig. 11, and nearly reproduces the trends of Cardamom Hill silicic charnockite samples. In Fig. 11, the least evolved samples of silicic charnockites are consistent with a partial melting model. The possibility of later fractional crystallization is supported by the trends of evolved samples. Here fractionation is still possible if assimilation of small amounts of crustal material is involved and is supported by the high Cr contents of evolved samples from the Cardamom Hill silicic charnockites.

Concluding remarks

A plausible model for the Cardamom Hill charnockites

Although their close spatial association and near continuous variations in major and trace element compositions point to a genetic link, separate petrogenetic scenarios are suggested for the older intermediate charnockites and younger silicic charnockites from the Cardamom Hill massif. It is argued that the composition of intermediate charnockites can be best explained in terms of interaction of mafic mantle derived magmas with crustal rocks via

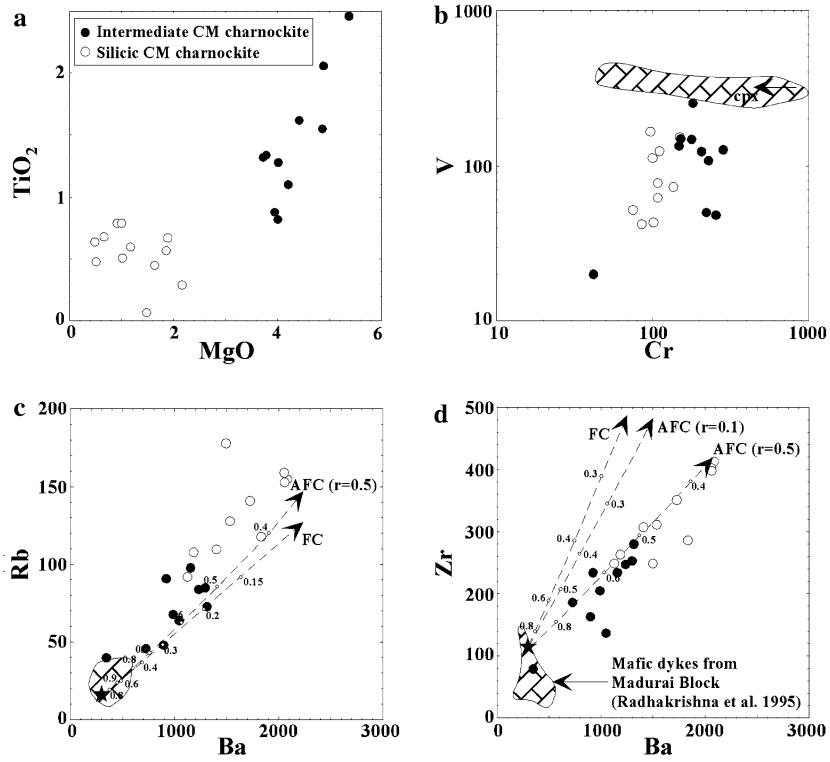

Fig. 9 **a** TiO_2 versus MgO plot, **b** V versus Cr plot, **c** Rb versus Ba plot, and **d** Zr versus Ba plot of the Cardamom Hill (CM) charnockite samples. The compositional ranges of mafic dykes from the Madurai block are also shown. Simple fractional crystallization (FC) models and assimilation fractional crystallization (AFC) models for a parental basaltic magma are shown in (**c**) and (**d**). The composition of the assimilant is the average of granodioritic hbl-bt gneiss (Rajesh 1999). The partition coefficients are from Arth (1976), Arth and Barker (1976), Henderson (1982), and Green and Pearson (1985)

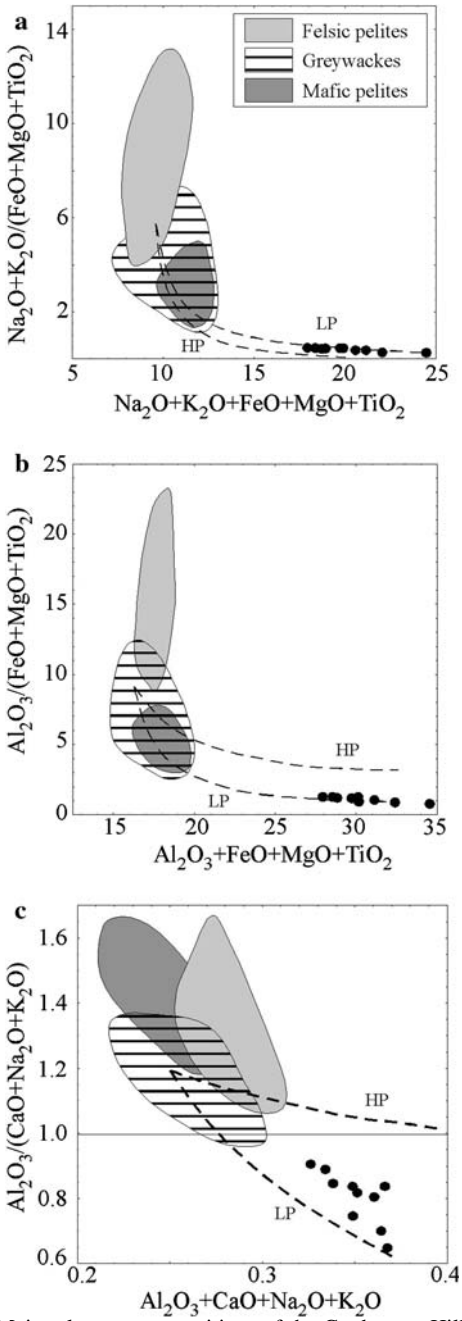

Fig. 10 Major element compositions of the Cardamom Hill intermediate charnockite samples plotted as a ratio between two variables versus the sum of the same variables. Compositions of melts generated experimentally by dehydration melting of felsic pelites, mafic pelites and greywackes are shown (see Patiño Douce 1999 for the compilation and source of data). The dashed lines are reaction curves that model the melt compositions that would be produced by hydridization of high-Al olivine tholeiite with metagreywacke (Patiño Douce 1999). *LP* low pressure; *HP* high pressure. All the values, except (c), are in wt%. In (c) illustrating alumina saturation relationships, the *y*-axis is molar alumina over alkalis plus lime and abscissa shows moles per 100 g of rock

AFC process. The high *r* factors of about 0.5 or greater, as required by AFC models, suggests that assimilation started at the very beginning of differentiation at relatively high

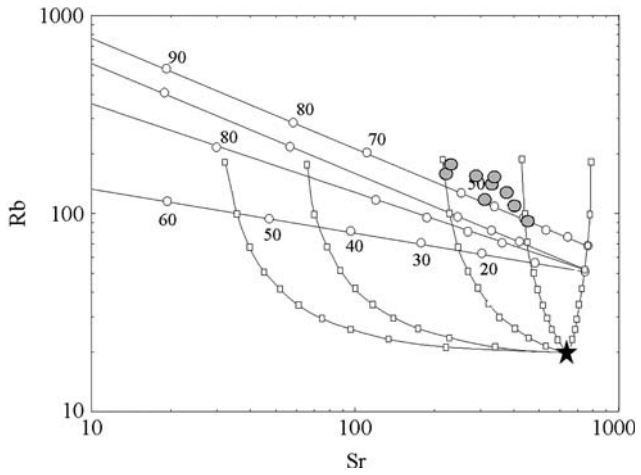

Fig. 11 Log Rb versus log Sr plot illustrating an initial partial melting and later fractional crystallization model for the Cardamom Hill silicic charnockites. The starting material is a hydrous basalt. Each *small box* and *circle* on the partial melting and fractional crystallization curves represent 10% of the amount of melting and residual liquid, respectively. The partition coefficients were taken from Thompson (1982) and Fujimaki et al. (1984)

temperatures and can be best explained in terms of reactive bulk assimilation (Beard et al. 2005). The calc-alkaline trend and continental arc tectonic setting of the intermediate charnockites are in line with the general notion that arc magmas commonly represent complex mixtures of mantle and crustal components including assimilation of crustal rocks by mafic magma (e.g., DePaolo 1981; Hildreth and Moorbath 1988; DePaolo et al. 1992; Spera and Bohrson, 2001).

Silicic charnockites on the other hand are high temperature melts of moderately hydrous basaltic magmas. A two-stage model which involves an initial partial melting of hydrous basaltic magma and later fractionation explains the geochemical features of the silicic charnockites, with the fractionation stage most probably an open system AFC. Considering the generation of the magma in a possible subduction-type tectonic setting, it is important to note that medium- to high-K basalts are common in subduction related magmatic arcs and are known to have water contents of up to 6 wt% (Sisson and Grove 1993; Roggensack et al. 1997). It is widely suggested that dehydration melts of greenstones and amphibolites are similar in composition to arc tonalities, and may account for the generation of silicic low-K arc magmas. Similarly, high temperature melts of hydrous basalt may account for the generation of silicic medium- to high-K arc magmas, like the Cardamom Hill silicic charnockite. Thus the occurrence of large silicic charnockites along continental margins probably indicates fertile mafic compositions like hydrous basalts within deeper portions of continental margin arcs.

Implications for charnockite magmatism in high-grade terrains

A compilation of geochemical data from the southern Indian charnockite massifs showed the possibility of two main compositional groups, intermediate (low-SiO_2) charnockites and silicic (high-SiO_2) charnockites, similar to the Cardamom Hill charnockites. Intermediate (low-SiO_2) charnockites are dominantly calc-alkalic to calcic (in terms of modified alkali-lime index) and predominantly magnesian (in terms of Fe-number), while silicic (high-SiO_2) charnockites are alkalic to alkali-calcic to calc-alkalic and predominantly ferroan (Fig. 12). The intermediate and silicic charnockites have quite different K_2O/Na_2O ratios, with the latter having a higher and extended range than the former. In general, intermediate charnockites fall mainly in the trondhjemite–tonalite fields, while the silicic charnockite compositions show an extended range up to the granite field in the normative An–Ab–Or plot. All the charnockite massifs from southern India are rich in Ba and Sr, similar to high-Ba–Sr granitoids (Tarney and Jones 1994), with the intermediate charnockites showing similarities to high-Ba–Sr granitoids with low K_2O/Na_2O ratios and the silicic charnockites showing similarities to high-Ba–Sr granitoids with high K_2O/Na_2O ratios.

Significantly the chemical composition of intermediate charnockites from southern India generally follow the reaction curves modeled by Patiño Douce (1999) to illustrate the interaction of a putative crustal melt end member with a basaltic melt, while the silicic charnockite compositions from southern India are broadly compatible with a hydrous basaltic source (not shown). Hence the above discussion on the petrogenetic characterization of intermediate and silicic charnockites from Cardamom hill massif can be of relevance in addressing the petrogenesis of other southern Indian charnockite massifs. Regarding the model for silicic charnockites, the deep seated crystallization of hydrous basaltic magmas differ from dehydration melting of the lower crust, as modeled by Petford and Gallagher (2001), in one fundamental regard, the availability of H_2O. In dehydration melting the H_2O content of the source rock is strictly limited by the amount of H_2O that can be structurally bound in hydrous minerals such as amphibole and mica. By contrast, deep-seated crystallization of hydrous arc basalt magmas has no such upper limit on H_2O content (e.g., Sisson and Layne 1993). The wide range of H_2O contents and bulk compositions of parental arc basalts ensures that crystallization of hydrous basalt can generate silicic melts like the silicic charnockites.

Application of the intermediate (low-SiO_2)–silicic (high-SiO_2) classification to selected charnockite occurrences from different parts of the world, did show positive results (Fig. 12). Here mangerites (opx-bearing monzonite) and quartz mangerites are an exception. In spite of their

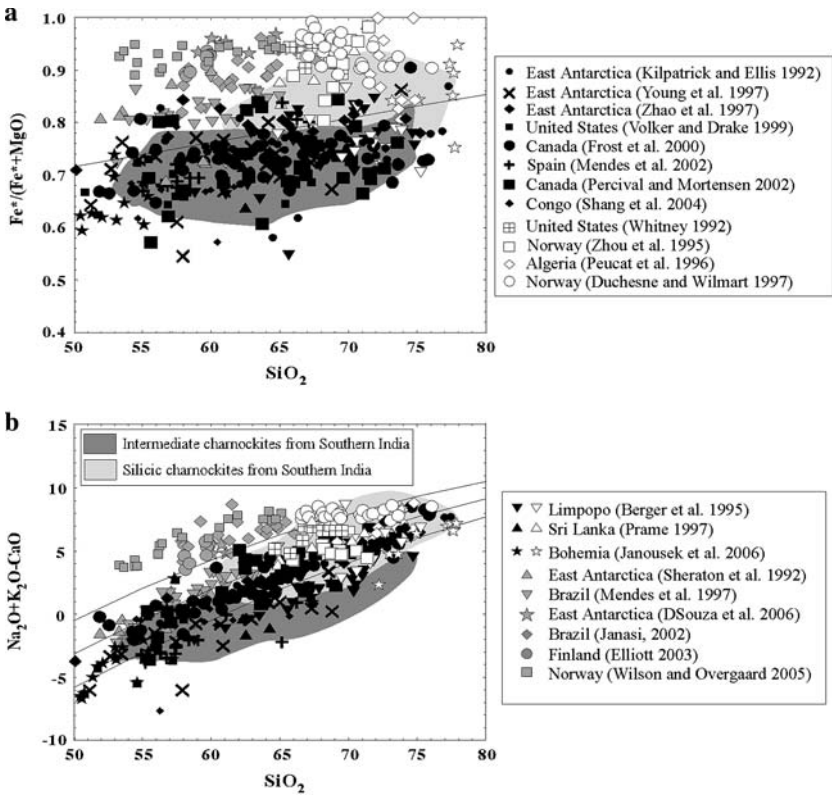

Fig. 12 Plots illustrating the application of intermediate-silicic classification to southern Indian charnockite massifs and selected charnockite occurrences worldwide. *Dark symbols* indicate intermediate charnockites and *open symbols* indicate silicic charnockites. Monzonitic/Qtz monzonitic samples are shown by *grey symbols*. **a** $Na_2O + K_2O$–CaO versus SiO_2 plot, **b** Fe*/Fe* + MgO versus SiO_2 plot

low-SiO_2, mangerites and quartz mangerites are alkali-calcic to alkalic and predominantly ferroan similar to silicic (high-SiO_2) charnockites (Fig. 12). Hence the compatibility of the intermediate-silicic classification should be treat with caution as a wide-range of rock compositions are grouped under the charnockite family (Le Maitre 2002). Nevertheless, the classification of charnockites into intermediate (low-SiO_2) and silicic (high-SiO_2) types can be of relevance in addressing the petrogenesis of charnockite massifs in high-grade terrains. It is suggested that for massifs showing spatial association of intermediate and silicic charnockites, a model taking into account of their compositional difference in terms of the effect of variations in the conditions (e.g., temperature, water fugacity) that prevailed, can account for plausible petrogenetic scenarios as illustrated for the Cardamom hill massif from southern India.

Acknowledgments Satish Hari assisted in fieldwork. Toshiaki Tsunogae, Yasuhito Osanai, John Akai, Teiichi Ueno, and Doyama are thanked for their hospitality, analytical facilities and discussions. James Beard and an anonymous reviewer provided thoughtful and encouraging comments on the manuscript. Some key references introduced by James Beard were helpful in clarifying aspects of the model presented in this manuscript. Editorial comments by Tim Grove were valuable. A JSPS visiting researcher fellowship (with Toshiaki Tsunogae) is acknowledged. This is a contribution to the Paleoproterozoic Mineralization (PPM) Research Group and Gondwana Institute for Geology and Environment (GIGE).

References

Arth JG (1976) Behavoir of trace elements during magmatic processes—a summary of theoretical models and their applications. J Res US Geol Surv 4:41–47

Arth JG, Barker F (1976) Rare-earth partitioning between hornblende and dacitic liquid and implications for the genesis of trondhjemitic–tonalitic magmas. Geology 4:534–536

Balaram V, Ramesh SL, Anjiah KV (1996) New trace element and REE data in thirteen GSF reference samples by ICP-MS. Geostand News Lett 20:71–78

Bartlett JM, Harris NBW, Hawkesworth CJ, Santosh M (1995) New isotope constraints on the crustal evolution of South India and Pan-African granulite metamorphism. Geol Soc India Mem 34:391–397

Beard JS, Lofgren GE (1991) Dehydration melting and water-saturated melting of basaltic and andesitic greenstones and amphibolites at 1, 3 and 6.9 kb. J Petrol 32:365–401

Beard JS, Ragland PC, Rushmer T (2004) Hydration crystallization reactions between anhydrous minerals and hydrous melt to yield amphibole and biotite in igneous rocks: description and implications. J Geol 112:617–621

Beard JS, Ragland PC, Crawford ML (2005) Reactive bulk assimilation: A model for crust–mantle mixing in silicic magmas. Geology 33:681–684

Berger M, Kramers JD, Nagler TF (1995) Geochemistry and geochronology of charnoenderbites in the Northern Marginal Zone of the Limpopo Belt, Southern Africa, and genetic models. Swiss Bull Miner Petrol 75:17–42

Bhaskar Rao YJ, Janardhan AS, Vijaya Kumar T, Narayana BL, Dayal AM, Taylor PN, Chetty TRK (2003) Sm-Nd model ages and Rb-Sr isotopic systematics of charnockites and gneisses across the Cauvery Shear Zone, Southern India: implications for the Archean–Neoproterozoic terrane boundary in the Southern Granulite Terrain. In: Ramakrishnan M (ed) Tectonics of Southern Granulite terrain: Kuppam–Palani Geotransect. Mem Geol Soc India 50:297–317

Bohlender F, van Reenen DD, Barton Jr JM (1992) Evidence for metamorphic and igneous charnockites in the southern Marginal zone of the Limpopo Belt. Precambrian Res 55:429–449

Centre for Earth Science Studies (2004) Report on deep continental studies (DCS) programme

Chacko T, Kumar GRR, Meen JK, Rogers JJW (1992) Geochemistry of high grade supracrustal rocks from the Kerala Khondalite Belt and adjacent massif charnockites. Precambrian Res 55:469–489

Condie KC, Allen P (1984) Origin of Archaean charnockites from southern India In: Kröner A, Hanson GN, Goodwin AM (eds) Archaean Geochemistry, Springer, Berlin, pp 183–203

Debon F, Le Fort P (1988) A cationic classification of common plutonic rocks and their magmatic associations: principles method applications. Bull Minéral 111:493–510

DePaolo DJ (1981) Trace element and isotopic effects of combined wall rock assimilation and fractional crystallization. Earth Planet Sci Lett 53:189–202

DePaolo DJ, Perry FV, Baldridge WS (1992) Crustal vs. mantle sources of granitic magmas: a two parameter model based on Nd isotopic studies Trans R Soc Edinb Earth Sci 83:439–446

Drummond MS, Defant MJ (1990) A model for trondhjemite–tonalite–dacite genesis and crustal growth via slab melting: Archaean to modern comparisons. J Geophys Res 95:21503–21521

D'Souza MJ, Keshava-Prasad AV, Ravindra R (2006) Genesis of ferropotassic A-type granitoids of MuhligHofmannfjella, Central Dronning Maud Land, East Antarctica. In: Contributions to global earth sciences. Springer, Berlin, pp 45–54

Duchesne J-C, Wilmart E (1997) Igneous charnockites and related rocks from the Bjerkreim-Sokndal layered intrusion (southwest Norway): a jotunite (hypersthene monzodiorite)-derived A-type granitoid suite. J Petrol 38:337–369

Duchesne J-C, Wilmart E, Demaiffe D, Hertogen J (1989) Monzonorites from Rogaland southwest Norway: a series of rocks coeval but no comagmatic with massif-type anorthosites. Precambrian Res 45:111–128

Eggins S, Hensen BJ (1987) Evolution of mantle-derived, augite-hypersthene granodiorites by crystal–liquid fractionation: Barrington Tops batholith, eastern Australia. Lithos 20:295–310

Elliott BA (2003) Petrogenesis of the post-kinematic magmatism of the central Finland granitoid complex II; Sources and magmatic evolution. J Petrol 44:1681–1701

Emslie RF (1991) Granitoids of rapakivi granite-anorthosite and related associations. Precambrian Res 51:173–192

Emslie RF, Hunt PA (1990) Ages and petrogenetic significance of igneous mangerite-charnockite suites associated with massif anorthosites, Grenville Province. J Geol 98:213–231

Frost BR, Frost CD, Hulsebosch TP, Swapp SM (2000) Origin of the charnockites of the Louis Lake Batholith, Wind River Range, Wyoming. J Petrol 41:1759–1776

Frost BR, Barnes CG, Collins WJ, Arculus RJ, Ellis DJ, Frost CD (2001) A geochemical classification for granitic rocks. J Petrol 42:2033–2048

Fujimaki H, Tatsumoto M, Aoki K (1984) Partition coefficients of Hf, Zr and REE between phenocrysts and ground masses. J Geophys Res 89:B662–B672

Ghosh JG, de Wit MJ, Zartman RE (2004) Age and tectonic evolution of Neoproterozoic ductile shear zones in the southern granulite

terrain of India, with implications for Gondwana studies. Tectonics 23 (TC3006)
Green TH, Pearson NJ (1985) Rare earth element partitioning between clinopyroxene and silicate liquid at moderate to high pressure. Contrib Miner Petrol 91:24–26
Green TH, Pearson NJ (1986) Ti-rich accessory phase saturation in hydrous mafic-felsic compositions at high P, T. Chem Geol 54:185–201
Grew ES (1984) Note on sapphirine and sillimanite + orthopyroxene from Panrimalai, Madurai district, Tamil Nadu. J Geol Soc India 25:116–119
Grove TL, Kinzler RJ, Baker MB, Donnelly-Nolan JM, Lesher CE (1988) Assimilation of granite by basaltic magma at Burnt Lava flow, Medicine Lake volcano, northern California: decoupling of heat and mass transfer. Contrib Miner Petrol 99:320–343
Hanson GN (1978) The application of trace elements to the petrogenesis of igneous rocks of granitic composition. Earth Planet Sci Lett 38:26–43
Harris NBW, Holt RW, Drury SA (1982) Geobarometry, geothermometry, and late Archean geotherms from granulite facies terrain of South India. J Geol 90:509–527
Harris NBW, Santosh M, Taylor PN (1994) Crustal evolution in South India: constraints from Nd isotopes. J Geol 102:139–150
Harrison TM, Watson EB (1984) The behavior of apatite during crustal anatexis: equilibrium and kinetic considerations. Geochim Cosmochim Acta 48:1464–1477
Helz RT (1976) Phase relations of basalts in their melting ranges at pH_2O = 5 kbar, part II: melt compositions. J Petrol 17:139–193
Henderson P (1982) Inorganic geochemistry. Pergamon Press, Oxford, pp 353
Hildreth W, Moorbath S (1988) Crustal contributions to arc magmatism in the Andes of central Chile. Contrib Miner Petrol 98:455–489
Icenhower JP, Dymek RF, Weaver BL (1998) Evidence for an enriched mantle source for jotunite (orthopyroxene monzodiorite) associated with the St. Urbain anorthosite, Quebec Lithos 42:191–212
Janasi VdA (2002) Elemental and Sr-Nd isotope geochemistry of two Neoproterozoic mangerite suites in SE Brazil: implications for the origin of the mangerite–charnockite–granite series. Precambrian Res 119:301–327
Janousek V, Gerdes A, Vrána S, Finger F, Erban V, Friedl G, Braithwaite CR (2006) Low-pressure granulites of the Lisov massif, southern Bohemia: Viséan metamorphism of late Devonian plutonic arc rocks. J Petrol 47 (available online)
Jayananda M, Peucat JJ (1996) Geochronological framework of southern India. In: Santosh M, Yoshida M (eds) The Archaean and Proterozoic terrains in southern India within East Gondwana. Gond Res Grp Mem 3:53–75
Jayananda M, Janardhan AS, Sivasubramanian P, Peucat J-J (1995) Geochronologic and isotopic constraints on the granulite formation in the Kodaikanal area, southern India. Geol Soc India Mem 34:373–390
Kilpatrick JA, Ellis DJ (1992) C-type magmas: igneous charnockites and their extrusive equivalents. Trans R Soc Edinb Earth Sci 83:155–164
Koshimoto S, Tsunogae T, Santosh M (2004) Sapphirine and corundum bearing ultrahigh temperature rocks from the Palghat–Cauvery Shear System, southern India. J Miner Petrol Sci 99:298–310
Lal RK, Ackermand D, Raith M, Raase P, Seifert F (1984) Sapphirine-bearing assemblages from Kiranur, southern India: a study of chemographic relationships in the Na_2O–FeO–MgO–Al_2O_3–SiO_2–H_2O system. Neu Jähr Min Abh 150:121–152
Le Maitre RW (ed) (2002) Igneous rocks: a classification and glossary of terms, Cambridge University Press, London
Le Roex AP (1985) Geochemistry, mineralogy and magmatic evolution of the basaltic and trachytic lavas from Gough island, South Atlantic. J Petrol 26:149–186
Longhi J, Vander Auwera J, Fram MS, Duchesne JC (1999) Some phase equilibrium constraints on the origin of Proterozoic (massif) anorthosites and related rocks. J Petrol 40:339–362
Markl G, Höhndorf A (2003) Isotopic constraints on the origin of AMCG-suite rocks on the Lofoten Islands, N Norway. Miner Petrol 78:149–171
Marsh JS (1989) Geochemical constraints on coupled assimilation and fractional crystallization involving upper crustal compositions and continental tholeittic magma. Earth Planet Sci Lett 92:70–80
Martin H (1986) Effect of steeper Archaean geothermal gradient on geochemistry of subduction zone magmas. Geology 14:753–756
Martin H (1987) Petrogenesis of Archaean trondhjemites, tonalites, and granodiorites from eastern Finland: major and trace element geochemistry. J Petrol 28:921–953
Mendes JC, Wiedemann CM, McReath I (2002) Norito e charnoenderbitos da borda do maciço intrusivo de Venda Nova, Espírito Santo. Anuário do Instituto de Geociências 25:99–124
Miller JS, Santosh M, Pressley RA, Clemens AS, Rogers JJW (1996) A Pan-African thermal event in southern India. J Southeast Asi Earth Sci 14:127–136
Mitchell JN, Scoates JS, Frost CD, Kolker A (1996) The geochemical evolution of anorthosite residual magmas in the Laramie anorthosite complex, Wyoming. J Petrol 37:637–660
Mohan A, Windley B (1993) Crustal trajectory of sapphirine-bearing granulites from Ganguvarpatti, South India: evidence for isothermal decompression path. J Met Geol 11:867–878
Mojzsis SJ, Devaraju TC, Newton RC (2003) Ion microprobe U-Pb age determinations on zircon from the late Archean granulite facies transition zone of southern India. J Geol 111:407–425
Montel JM, Vielzeuf D (1997) Partial melting of metagreywackes, Part II. Compositions of minerals and melts. Contrib Miner Petrol 128:176–196
Newton RC, Smith JV, Windley BF (1980) Carbonic metamorphism granulites and crustal growth. Nature 288:45–50
Nielsen RL (1990) Simulation of igneous differentiation processes. In: Nicholls J, Russell JK (eds) Modern methods of igneous petrology: understanding magmatic processes. Rev Miner 24:65–105
Patiño Douce AE (1999) What do experiments tell us about the relative contributions of crust and mantle to the origin of granitic magmas? In: Castro A, Fernandez C, Vigneresse JL (eds) Understanding granites: integrating new and classical techniques. Geol Soc Sp Pub 168:55–75
Percival JA, Mortensen JK (2002) Water-deficient calc-alkaline plutonic rocks of northeastern Superior Province, Canada: significance of charnockitic magmatism. J Petrol 43:1617–1650
Petford N, Atherton M (1996) Na-rich partial melts from newly underplated basaltic crust: the Cordillera Blanca batholith. J Petrol 37:1491–1521
Petford N, Gallagher K (2001) Partial melting of mafic amphibolitic lower crust by periodic influx of basaltic magma. Earth Planet Sci Lett 193:483–439
Peucat J-J, Capdevila R, Drareni A, Choukroune P, Fanning CM, Bernard-Griffiths J, Fourcade S (1996) Major and trace element geochemistry and isotope (Sr, Ns, Pb, O) systematics of an Archaean basement involved in a 2.0 Ga very high temperature (1000°C) metamorphic event: In Ouzzal massif, Hoggar, Algeria. J Meta Geol 14:667–592
Prame WKBN (1997) Geochemistry and genesis of granitoid rocks from southern Sri Lanka. Miner Petrol 60:245–265
Radhakrishna T, Pearson DG, Mathai J (1995) Evolution of Archaean southern Indian lithospheric mantle: a geochemical study of

Proterozoic Agali-Coimbatore dykes. Contrib Miner Petrol 121:351–363

Raith M, Karmakar S, Brown M (1997) Ultrahigh temperature metamorphism and multistage decompressional evolution of sapphirine granulites from the Palni Hill ranges, South India. J Met Geol 15:379–399

Raith M, Srikantappa C, Buhl D, Kühler H (1999) The Nilgiri Enderbites, South India: nature and age constraints on protolith formation, high-grade metamorphism and cooling history. Precambrian Res 98:129–150

Rajesh HM (1999) Characterization and origin of alkaline and calc-alkaline aluminous A-type granitoids from southwestern India: implications for Gondwanaland tectonics. Unpublished DSc thesis Osaka City University Japan 317p

Rajesh HM (2004) The igneous charnockite—high-K alkali-calcic I-type granite—incipient charnockite association in Trivandrum Block, southern India. Contrib Miner Petrol 147:346–362

Rapp RP, Watson EB (1995) Dehydration melting of metabasalt at 8–32 kbar: implications for continental growth and crustmantle recycling. J Petrol 36:891–931

Rapp RP, Watson EB, Miller CF (1991) Partial melting of amphibolite/eclogites and the origin of Archean trondhjemites and tonalites. Precambrian Res 51:1–25

Reiners PW, Nelson BK, Ghiorso MS (1995) Assimilation of felsic crust by basaltic magma: thermal limits and extents of crustal contamination of mantle-derived magmas Geology 23:563–566

Roggensack K, Hervig RL, McNight SB, Williams SN (1997) Explosive basaltic volcanism from Cerro Negro volcano: influence of volatiles on eruptive style. Science 277:1639–1642

Rushmer T (1991) Partial melting of two amphibolites: contrasting experiment results under fluid absent conditions. Contrib Miner Petrol 107:41–59

Sajeev K, Osanai Y, Santosh M (2004) Ultrahigh-temperature metamorphism followed by two-stage decompression of garnet–orthopyroxene– sillimanite granulites from Ganguvarpatti, Madurai Block, southern India. Contrib Mineral Petrol 148:29–46

Santosh M (1996) The Trivandrum and Nagercoil granulite blocks. Gondwana Res Group Mem 3:243–277

Santosh M, Yokoyama K, Sekhar BS, Rogers JJW (2003) Multiple tectonothermal events in the granulite blocks of southern India revealed from EPMA dating: implications on the history of supercontinents. Gond Res 6:29–63

Satish-Kumar M, Wada H, Santosh M (2002) Constraints on the application of carbon isotope thermometry in high- to ultrahigh-temperature metamorphic terranes. J Meta Geol 20:335–350

Scoates JS, Lindsley DH (2000) New insights from experiments on the origin of anorthosite. EOS 81: F1300

Scoates JS, Frost CD, Mitchell JN, Lindsley DH, Frost BR (1996) Residual liquid origin for a monzonitic intrusion in a mid-Proterozoic anorthosite complex: the Sybille intrusion, Laramie Anorthosite Complex, Wyoming. Geol Soc Am Bull 108:1357–1371

Shang CK, Satir M, Siebel W, Nsifa EN, Taubald H, Liégeois JP, Tchoua FM (2004) TTG magmatism in the Congo craton; a view from major and trace element geochemistry, Rb–Sr and Sm–Nd systematics: case of the Sangmelima region, Ntem complex, southern Cameroon. J Afr Earth Sci 40:61–79

Sheraton JW, Black LP, Tindle AG (1992) Petrogenesis of plutonic rocks in a Proterozoic granulite-facies terrane–the Bunger Hills, East Antarctica. Chem Geol 97:163–198

Sisson TW, Grove TL (1993) Experimental investigations of the role of H_2O in calc-alkaline differentiation and subduction zone magmatism. Contrib Miner Petrol 113:143–166

Sisson TW, Layne GD (1993) H_2O in basalt and basaltic andesite glass inclusions from four subduction-related volcanoes. Earth Planet Sci Lett 117:619–635

Sisson TW, Ratajeski K, Hankins WB, Glazner AF (2005) Voluminous granitic magmas from common basaltic sources. Contrib Miner Petrol 148:635–661

Spera FJ, Bohrson WA (2001) Energy-constrained open system magmatic processes I: general model and energy-constrained assimilation and fractional crystallization (EC-AFC) formulation J Petrol 42:999–1018

Springer W, Seck HA (1997) Partial fusion of basic granulites at 5 to 15 kbar: implications for the origin of TTG magmas. Contrib Miner Petrol 127:30–45

Tarney J, Jones CE (1994) Trace element geochemistry of orogenic igneous rocks and crustal growth models. J Geol Soc Lond 151:855–868

Thompson RN (1982) British Tertiary volcanic province. Scott J Geol 18:49–107

Vander Auwera J, Longhi J, Duchesne JC (1998) A liquid line of descent of the jotunite (hypersthene monzodiorite) suite. J Petrol 39:439–468

Verma SP, Guevara M, Agarwal S (2006) Discriminating four tectonic settings: Five new geochemical diagrams for basic and ultrabasic volcanic rocks based on log-ratio transformation of major element data. J Earth Sys Sci 115:485–528

Volker RA, Drake Jr AA (1999) Geochemistry and stratigraphic relations of middle Proterozoic rocks of the New Jersey Highlands. US Geol Surv Prof Pap 1565

Wendlandt RF (1981) Influence of CO_2 on melting of model granulite facies assemblages: a model for the genesis of charnockites. Am Miner 66:1164–1174

Whitney PR (1992) Charnockites and granites of the western Adirondacks, New York, USA: a differentiated A-type suite. Precambrian Res 57:1–19

Wilson JR, Overgaard G (2005) Relationship between the Layered Series and the overlying evolved rocks in the Bjerkreim-Sokndal Intrusion, southern Norway. Lithos 83:277–298

Wolf MB, Wyllie PJ (1989) The formation of tonalitic liquids during the vapor-absent partial melting of amphibolite at 10 kbar. EOS 70:506

Wolf MB, Wyllie JP (1994) Dehydration melting of amphibolite at 10 kbar: the effects of temperature and time. Contrib Miner Petrol 115:309–383

Young DN, Zhao J–X, Ellis DJ, McCulloch MT (1997) Geochemical and Sr-Nd isotopic mapping of source provinces for the Mawson charnockites East Antarctica: implications for Proterozoic tectonics and Gondwana reconstructions. Precambrian Res 86:1–19

Zhao J-X, Ellis DJ, Kilpatrick JA, McCulloch MT (1997) Geochemical and Sr-Nd isotopic study of charnockites and related rocks in the northern Prince Charles Mountains East Antarctica: implications for charnockite petrogenesis and Proterozoic crustal evolution. Precamb Res 81:37–66

Zhou XQ, Bingen B, Demaiffe D, Liégois J–P, Hertogen J, Weis D, Michot J (1995) The 1160 Ma Hidderskog meta-charnockite: implications of this A-type pluton for the Sveconorwegian belt in SW Norway. Lithos 36:51–66